IEEE Access
Multidisciplinary | Rapid Review | Open Access Journal

Received December 26, 2020, accepted January 3, 2021, date of publication January 8, 2021, date of current version January 21, 2021.

Digital Object Identifier 10.1109/ACCESS.2021.3049789

A Novel Adaptive Fault Diagnosis Method for Wind Power Gearbox

NENGQUAN DUAN[1], JINGTAI WANG[2], TIANSHENG ZHAO[3], WENHUA DU[1], XIAOMING GUO[4], AND JUNYUAN WANG[1]

[1]Shanxi Province Key Laboratory of Advanced Manufacturing Technology, North University of China, Taiyuan 030051, China
[2]Taiyuan Heat Group Company Ltd., Taiyuan 030001, China
[3]Zhengzhou Mechanical and Electrical Engineering Institute, Zhengzhou 450015, China
[4]School of Mechanical Engineering, North University of China, Taiyuan 030051, China

Corresponding author: Junyuan Wang (wangyi01161013@163.com)

This work was supported in part by the National Natural Science Foundation of China under Grant 51905496, in part by the Shanxi Provincial Natural Science Foundation of China under Grant 201801D121186 and Grant 201801D221237, in part by the Science Foundation of the North University of China under Grant XJJ201802, in part by the Shanxi Provincial Key Laboratory Open Foundation of China under Grant XJZZ201802, in part by the Science and Technology Development Center of the Ministry of Education University Industry-University-Research Innovation Fund under Grant 2018C01050, and in part by the Shanxi Province Applied Basic Research Project of China under Grant 201701D121061.

ABSTRACT In the noisy environment, fault characteristics of the composite faults of the wind power gearbox are coupled with each other, which makes the extraction features more difficult. In order to extract the characteristics of composite faults, a new fault diagnosis method for wind power gearbox is proposed in this paper, namely the modified Savitzky Golay Laplacian of Gaussian filter (MSGloG). The method can not only solve the defects that the scale parameters of the Modified Laplacian of Gaussian filter (MloG) filter are not adaptive, but also overcome the problems that the smoothing effect is too much affected by noise. Firstly, determining the Laplace model of Gaussian filter, and using the least square convolution smoothing process to improve the signal-to-noise ratio of the vibration signal. Secondly, a new marginal envelope spectrum entropy index is proposed to measure the complex fault characteristics. Finally, a new chaotic grey wolf optimization algorithm is proposed, which uses the marginal envelope spectral entropy as the fitness function, and the purpose is to make the MSGloG noise reduction adaptive. The method extracted the faults of the bearing outer ring and rolling elements successfully.

INDEX TERMS Wind power gearbox, fault diagnosis, modified Savitzky Golay Laplacian of Gaussian filter, marginal envelope spectral entropy.

I. INTRODUCTION

The extraction of fault features in gearboxes in a strong noise environment has always been a difficult point in fault diagnosis research [1]–[4]. The international research on wind turbine gearbox fault feature extraction has been carried out in many aspects. The fault feature identification of wind turbine gearbox mainly includes fault classification and fault feature extraction [5]–[8]. For the fault feature extraction, due to the harsh working environment of the wind turbine gearbox, various wind loads will cause different degrees of damage to the wind turbine gearbox bearings. The characteristic signal of fault mainly exists in the form of periodic impact, and the impact signal usually contains a lot of noise, which poses a certain challenge to the feature extraction of early fault. Therefore, it is especially important to research a high-efficiency and high-precision fault diagnosis method for wind turbine gearboxes.

Traditional noise reduction methods include linear filtering techniques and nonlinear filtering techniques [7]. Linear filtering has always played an important role in the filtering field because of its perfect theoretical foundation, simple mathematical processing, easy to adopt FFT and hardware implementation. It has a good smoothing effect on Gaussian noise, but it has a poor suppression effect on pulse signals and other forms of high-frequency components, which is prone to distortion. Nonlinear filtering is based on a nonlinear mapping relationship of the input signal sequence. It can often

The associate editor coordinating the review of this manuscript and approving it for publication was Baoping Cai.

map a specific noise to zero and preserve the important characteristics of the signal, which can overcome the deficiency of the linear filter to some extent.

In recent years, many new denoising methods have emerged, such as Laplacian score [9], fuzzy theory [10], morphology filtering [11], deconvolution algorithm filtering [12], [13] and decomposition method [14]–[17]. Wiggins [18] first applied MED to the fault diagnosis of rotating machinery, because its filter size needs to be manually set, the algorithm has certain limitations. On this basis, Cheng *et al.* [19] optimize the particle swarm optimization of parameters in MED to make it adaptive and a combination of deconvolution method and modal decomposition method was developed to extract the composite fault features. Cheng *et al.* [20] combined the ensemble empirical modal decomposition (EEMD) and MED to extract the fault features effectively, but the MED can only extract a single pulse. McDonald *et al.* [21] propose the MOMEDA to extract the fault features. MOMEDA can obtain the optimal filter without iteration, eliminates the error generated by iteration, and can effectively extract the periodic pulse. Wang *et al.* [22] optimize the filter length of MOMEDA through the grid search algorithm to make it adaptive and effectively extracts the characteristics of single bearing faults in the gearbox. Gaussian noise is a kind of common noise, and the corresponding Gaussian filtering overcomes the traditional filtering phase shift and complex design defects, as a zero-phase-shift filtering method with the smallest time-frequency window area [23], autoregressive filter (AR) [24] has received extensive attention in the field of signal processing, it has good performance in time series analysis, signal modelling, etc. At present, the Gaussian filtering method is mainly applied to the edge processing of images [25], and little research has been done on the fault diagnosis of rotating machinery. For its excellent filtering performance, this paper uses its fault diagnosis for wind turbine gearbox. However, the traditional Gaussian filter is not adaptive due to the parameter determination problem, and it is easy to smooth out the mutation information when performing fault diagnosis of the wind power gearbox under different working conditions.

In recent years, intelligent algorithms have flourished and have been widely used in parameter optimization. Among them, the grey wolf optimization algorithm (GWO) [26] is a new meta-heuristic algorithm based on grey wolf predation behavior, and it has been proved to be a high-level exploration and development algorithm. But there are problems with development and exploration imbalances so that their performance is not ideal [27]. In order to make the determined Gaussian filter parameters more reasonable, a chaotic grey wolf algorithm (CGWO) with marginal envelope spectral entropy as the fitness function is proposed for iterative selection. The principle is to introduce chaos theory into GWO, to balance the exploration and development of GWO, increase individual diversity, increase the probability of jumping out of local optimal solution and explore the solution space in depth.

The main contributions of this work are as follows:1) An adaptive Gaussian filtering method is proposed and applied to the fault feature extraction of wind turbine gearbox for the first time; 2) In this work, this paper studies the filtering characteristics of MSGLoG and analyzes the influencing factors of its noise reduction characteristics. It optimizes the parameters through the chaotic grey wolf algorithm and highlights the advantages of extracting multiple fault features simultaneously. 3) Through the analysis of simulation signals and experimental signals, the effectiveness of the proposed fault diagnosis method is proved.And through the comparison with MED, MOMEDA and autoregressive filtering method AR, the advantages of the proposed method are further highlighted.

II. MODIFIED SAVITZKY GOLAY LAPLACIAN OF GAUSSIAN FILTER

Marr and Hildreth [28] proposed a Laplacian Gaussian filter to detect the abrupt change of the vibration signal by smoothing the background noise. The coefficient of the LoG filter can be obtained by determining the second derivative of the Gaussian filter. Eq. (1) is a first-order Gaussian filter.

$$G(n) = \frac{1}{\sqrt{2\pi}\sigma} \cdot e^{\left(\frac{-n^2}{2\sigma^2}\right)} \tag{1}$$

where the first parameter n is the mean of the random variable and the second parameter σ^2 is the variance of the random variable. Derived from Eq. (1) to get Eq. (2).

$$G'(n) = \frac{-1}{\sqrt{2\pi}} \cdot \frac{n}{\sigma^3} \cdot e^{\left(\frac{-n^2}{2\sigma^2}\right)} \tag{2}$$

Deriving Eq. (2) to obtain an LoG filter, as shown in Eq. (3).

$$G''(n) = \frac{1}{\sqrt{2\pi}} \cdot \frac{1}{\sigma^2} \cdot \left(\frac{n^2}{\sigma^2} - 1\right) \cdot e^{\left(\frac{-n^2}{2\sigma^2}\right)} \tag{3}$$

Normalize the LoG filter as shown in Eq. (4).

$$LoGFilter_{Normalized} = \frac{\frac{1}{\sqrt{2\pi}} \cdot \frac{1}{\sigma^2} \cdot \left(\frac{n^2}{\sigma^2} - 1\right) \cdot e^{\left(\frac{-n^2}{2\sigma^2}\right)}}{\sum_n e^{\left(\frac{-n^2}{2\sigma^2}\right)}} \tag{4}$$

LoG filter can be considered as a noise reduction technology for vibration signals, it is a kind of FIR filter. For FIR filters, when the sum of the filter coefficients tends to zero, it is a high-pass filter. And the high-pass FIR filter will not respond in the low frequency and zero frequency situations, which can effectively enhance the detailed information of the vibration signal. Therefore, this paper improves the formula of the LoG filter to make it a high-pass filter, as shown in Eq. (5).

In this paper, the final formula of the LoG filter is called the Modified Savitzky Golay Laplacian of Gaussian filter

(MSGloG).

$$\mathrm{MSGloG} = \frac{\frac{1}{\sqrt{2\pi}} \cdot \frac{1}{\sigma^2} \cdot (\frac{n^2}{\sigma^2} - 1) \cdot e^{\left(\frac{-n^2}{2\sigma^2}\right)}}{\sum_n e^{\left(\frac{-n^2}{2\sigma^2}\right)}} - \frac{1}{C} \sum_n \frac{\frac{1}{\sqrt{2\pi}} \cdot \frac{1}{\sigma^2} \cdot (\frac{n^2}{\sigma^2} - 1) \cdot e^{\left(\frac{-n^2}{2\sigma^2}\right)}}{\sum_n e^{\left(\frac{-n^2}{2\sigma^2}\right)}} \quad (5)$$

In Eq. (5), C denotes the filter order of the MSGloG filter. MSGloG filter is used for filtering processing of vibration signal. Every M sampling point near x in the original data are taken and x is set as the origin. Constructs an array of windows containing 2M+1 sample points centred on x, and constructs an i-order polynomial to fit the array:

$$p(n) = \sum_{k=0}^{i} a_k \cdot n^k \quad (6)$$

among them $-M \leq n \leq M, i \leq 2M + 1$;

The fitted residual is:

$$\varepsilon = \sum_{n=-M}^{M} (p(n) - x(n))^2 = \sum_{n=-M}^{M} (\sum_{k=0}^{i} a_k \cdot n^k - x(n))^2 \quad (7)$$

To obtain the minimum value of ε, the partial derivative of each parameter is 0.

$$\frac{\partial \varepsilon}{\partial a_i} = \sum_{n=-M}^{M} 2n^i (\sum_{k=0}^{N} a^k \cdot n^k - x[n])^2 \quad (8)$$

Obtain:

$$\sum_{k=0}^{N} (\sum_{n=-M}^{M} n^{i+k}) a_k = \sum_{n=-M}^{M} n^i x[n] \quad (9)$$

Move the filter of this window until you get all the fit points of the original data.

Gaussian filters have been widely used in many image processing fields, such as the field of edge detection [29]. The algorithm is sensitive to image abrupt changes; it can easily detect image edges. Because of its good filtering performance in image processing, this paper analyzes its performance in the fault diagnosis of wind turbine gearboxes, and it smoothed the filtered signal to enhance the weak vibration signal and improve the accuracy of fault diagnosis.

This paper proposes a new Gaussian Laplacian transform filtering method for gearbox fault diagnosis. The algorithm smoothest the background noise so that it is greatly reduced by the influence of noise. When the acquired vibration signal is processed using the MSGloG filter, the scale parameter σ and the filter order k have a large influence on the filtering performance. Firstly, when the scale parameter σ is too large, the fault information is easily misdiagnosed, and the fault information cannot be effectively identified, which reduces the accuracy and efficiency of fault diagnosis. Secondly, When σ is small, the diagnostic accuracy of fault features is low, the weak fault feature cannot be effectively extracted. Finally, in order to specify the influence of the scale parameter σ on the performance of the MloG filter, a set of simulation models is constructed to analyze the fault information. The main form of the fault information is a cyclical shock signal, so the simulated signal constructed is as follows:

$$\begin{aligned} x_1(t) &= A_{m1} \times \exp(-\frac{g}{T_{m1}}) \sin(2\pi f_a t) \\ x_2(t) &= A_{m2} \times \exp(-\frac{g}{T_{m2}}) \sin(2\pi f_a t) \\ x_3(t) &= x_1(t) + x_2(t) + noise \end{aligned} \quad (10)$$

Among them, $x(t)$ is a periodic impact signal. A_{m1} and A_{m2} represent the amplitude of the pulse, g is the damping coefficient, T_{m1} and T_{m2} are the periods of the impact, and f_a is the natural frequency of the axis. The parameter is set to: $g = 0.1, T_{m1} = 1/23, T_{m2} = 1/30, f_a = 320Hz$.

The simulation diagram constructed is shown in Figure 1. In this Figure, Figure1(a) is the waveform diagram of the first bearing fault, Figure 1(b) is the second fault characteristic information, and Figure 1(c) is the composite waveform of two faults and noise.

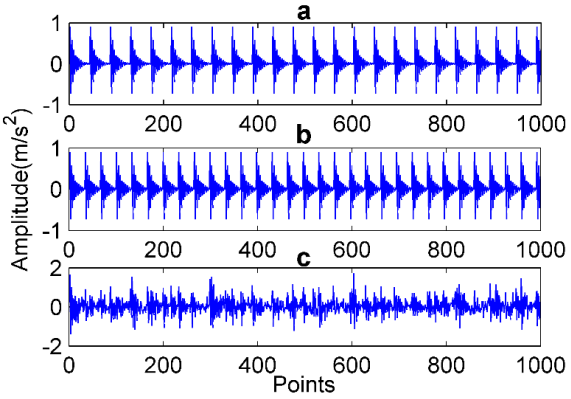

FIGURE 1. Multi-impact simulation signal diagram.

In order to explain the influence of the scale parameter σ on the MloG filter, three filters with σ of 0.7, 0.9 and 1.5 are respectively constructed to filter the simulation model. When analyzing the influence of the scale parameter σ on the performance of the MloG filter, this paper adopts the control variable method, select the length m of the sliding window to be a fixed value. It can be seen from Figure 2 that only the 30 Hz fault can be effectively extracted in the envelope spectrum obtained by filtering at $\sigma = 0.7$, and the fault with the fault frequency of 23 Hz is not effectively extracted, in the Figure, Figure2(a) is a composite image of multiple faults and noise, Figure 2(b) is a result map of filtering fault information by MloG, and Figure 2(c) is an envelope spectrum analysis diagram of the vibration signal after MloG filtering. It can be seen from Figure 3 that when $\sigma = 0.9$, the 23 Hz fault feature and the 30 Hz fault feature are effectively extracted, Figure 3(a) is a multi-fault and noise composite image, and Figure 3(b) is a result graph after filtering the fault information by MloG, Figure 3(c) is The envelope spectrum analysis diagram of the MloG filtered vibration signal is performed.

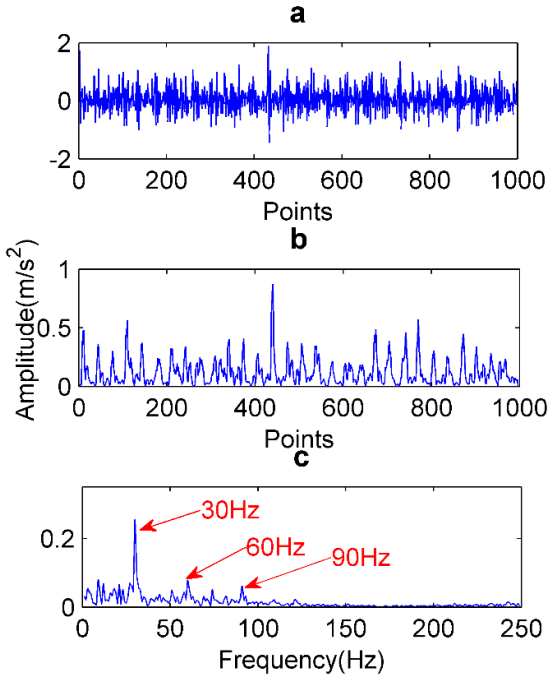

FIGURE 2. MloG extraction diagram of simulated signal at σ =0.7.

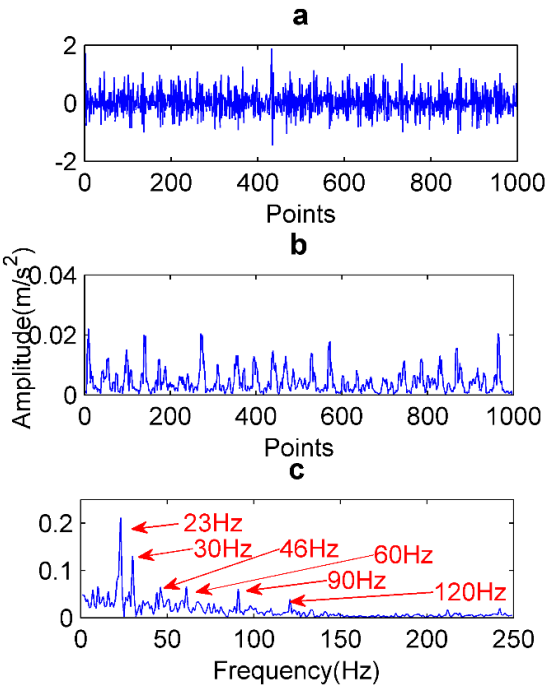

FIGURE 3. MloG extraction diagram of simulated signal at σ =0.9.

It can be seen from Figure 4 that when $\sigma = 1.5$, both fault information is effectively extracted, but in the envelope spectrum analysis result, it can be intuitively found that the frequency doubling information has a certain reduction compared with $\sigma = 0.9$, Figure 4(a) is a composite image with multiple faults and noise, Figure 4(b) is the resulting map after filtering the fault information by MloG, and Figure 4(c) is an envelope spectrum analysis graph of the vibration signal after MloG filtering. In summary, when the value of σ is too small, the multi-fault feature is not effectively extracted, and even a fault feature information may be extracted to cause missed diagnosis. Therefore, a reasonable scale parameter σ is especially important for the performance of the MloG filter.

When the vibration information is collected for the wind turbine gearbox since the working conditions contain a large amount of noise, the smoothing effect of the signal plays an important role in the accurate extraction of the fault information. The signal smoothing method MSGloG filter is newly constructed. The newly constructed MSGloG filter is essentially a least-square convolution smoothing, which is comprehensively considered according to the polynomial fitting order and the number of smoothing times.

In this paper, the advantages and disadvantages of smoothness performance are compared by constructing two groups of signals with different noise intensity. The constructed signal is shown in Eq. (11).

$$\begin{aligned} x_1(t) &= A_{m1} \times \exp(-\frac{g}{T_{m1}}) \sin(2\pi f_a t) \\ x_2(t) &= x_1(t) + noise \end{aligned} \tag{11}$$

Among them, $x(t)$ is a periodic impact signal. A_{m1} represent the amplitude of the pulse, g is the damping coefficient,

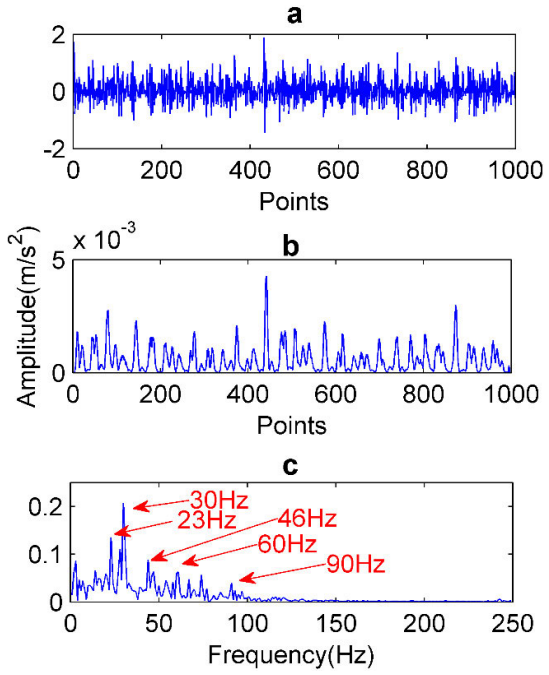

FIGURE 4. MloG extract diagram of simulated signal at σ =1.5.

T_{m1} is the periods of the impact, and f_a is the natural frequency of the axis. The parameter is set to: $g = 0.1, T_{m1} = 1/20, f_a = 260Hz$.

Figure 5 is a comparison of the smoothing performance of MloG and MSGloG at a signal-to-noise ratio of -10.1 dB. Figure 5 (a) is a fault signal composed of a shock signal and noise; Figure 5(b) shows the vibration signal after smoothing by MloG. The signal after smoothing by MloG has an intuitive reduction in amplitude; Figure 5(c) shows the vibration

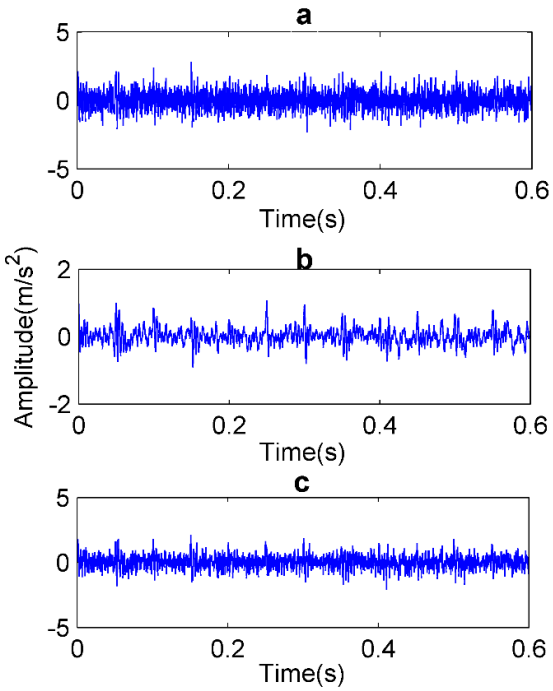

FIGURE 5. The time-domain comparison between MloG and MSGloG under −10.1dB SNR.

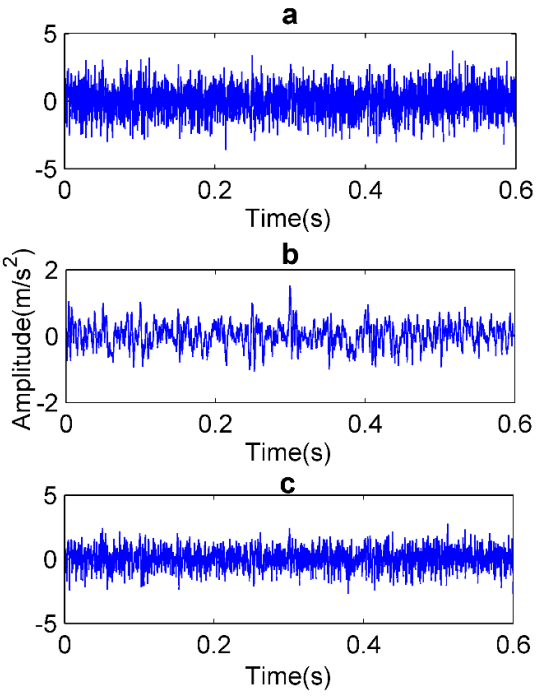

FIGURE 6. The time-domain comparison between MloG and MSGloG under −15.4dB SNR.

signal after smoothing by MSGloG, by calculating the signal-to-noise ratio of the signal in Figure 5(c) is -4.46dB, which is less than the original signal's SNR of -10.1dB. Figure 7 is a frequency domain result after smoothing MloG and MSGloG at a signal-to-noise ratio of -10.1 dB. Figure 7(a) is the signal envelope map after MloG smoothing and Figure 7(b) is the signal envelope map after MSGloG smoothing. The multiplier information can be clearly seen in both Figures, and the smoothing processing of MloG and MSGloG is effective under the signal-to-noise ratio of -10.1dB. Figure.6 is a time-domain diagram of the smoothing effect of MloG and MSGloG with a signal-to-noise ratio of −15.4dB. Figure 6(a) is the original vibration signal diagram constructed; Figure 6(b) shows the smoothed signal diagram after MloG processing for the signal with −15.4dB SNR; Figure 6(c) shows the smoothed signal diagram after MSGloG processing for the signal with −15.4dB SNR. Figure 8 is the result of envelope spectrum analysis of the signal with a signal-to-noise ratio of −15.4dB. Figure 8(a) is the signal envelope map after MloG smoothing processing. In this Figure, only the first peek of the fault characteristic frequency of 20 Hz can be extracted, and there is no effective multiplier, which cannot be used as the basis for fault feature extraction. Figure 8(b) is the signal envelope map after MSGloG smoothing. In this Figure, the fault frequency of 20 Hz and its multiplication information can be clearly seen, and the fault feature information can be effectively extracted.

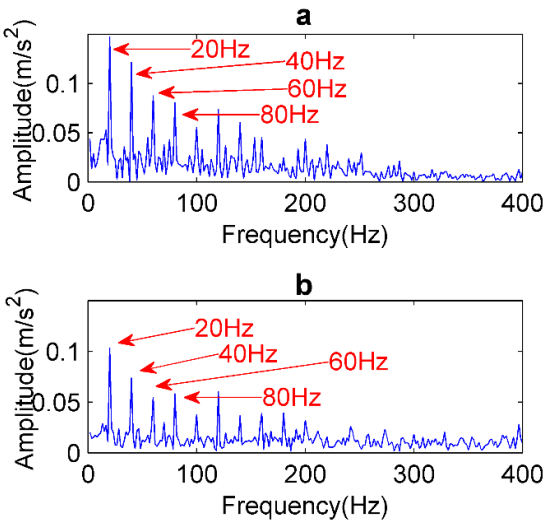

FIGURE 7. The frequency-domain comparison between MloG and MSGloG under −10.1dB SNR.

III. THE PROPOSED ADAPTIVE GAUSSIAN FILTER

In this paper, the adaptive MSGloG filtering method based on CGWO is proposed for the first time and applied to the extraction process of fault characteristics of wind turbine gearbox. In order to make the selected parameters optimal, the selection of the objective function and the application of the optimization algorithm are particularly important. The accurate objective function can select parameters with high efficiency and high precision.

A. PROPOSAL OF A NEW TYPE OF INDICATOR (MBLS)

Aiming at the defect that the selection of scale parameter σ and order k of MSGlog filter is not adaptive, a chaotic Gray Wolf algorithm is proposed to optimize MSGlog in this paper. Because the proposed method is mainly used in the fault

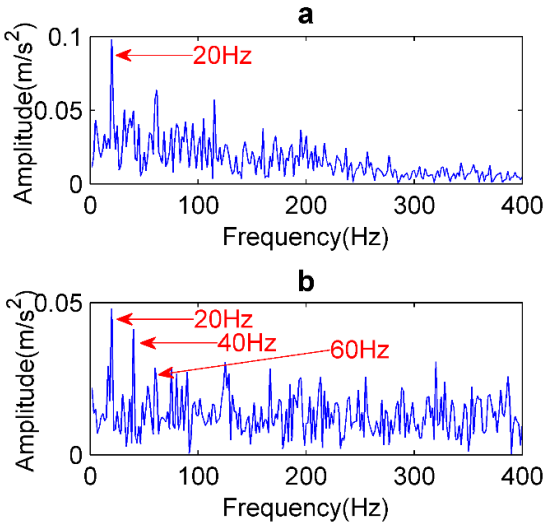

FIGURE 8. The frequency-domain comparison between MIoG and MSGIoG under −15.4dB SNR.

diagnosis of wind turbine gearbox under strong noise conditions, and the vibration signal is mainly represented by periodic pulse signal, therefore, in the process of MSGIoG adaptive optimization, the proposed fitness function should have the ability to characterize its noise reduction performance and highlight periodic pulses. Therefore, the marginal envelope spectral entropy (MBLS) is proposed to evaluate the noise reduction performance of the adaptive MSGIoG filter.

The marginal envelope spectral entropy is shown in Eq. (12).

$$MBLS = \frac{x_p}{\left(\frac{1}{N}\sum_{i=1}^{N}\sqrt{|x_i|}\right)^2 \cdot \frac{1}{\ln N}\sum_{i=1}^{N} p_i \cdot \ln p_i} \tag{12}$$

The envelope spectrum entropy and marginal index are included in this formula, where Eq. (13) is the calculation formula of the envelope spectral entropy and Eq. (14) is the calculation formula of the marginal index.

$$H_e = -\frac{1}{\ln N}\sum_{i=1}^{N} p_i \cdot \ln p_i \tag{13}$$

where P_i denotes the proportion of the spectral value of the i-th point of the envelope spectral entropy in the whole spectrum, and $i = 1, 2, \ldots, n$, n is the number of envelope spectral points.

$$MI = \frac{x_p}{\left(\frac{1}{N}\sum_{i=1}^{N}\sqrt{|x_i|}\right)^2} \tag{14}$$

where, $x_p = E[\max\{x(n)\}]$, N is the length of the signal.

Envelope spectral entropy is an indicator that can evaluate the periodicity of shock signals. Its basic idea is: firstly, the envelope of the original time-domain signal of the rolling bearing is extracted by Hilbert transform; secondly, the envelope signal is fast Fourier transformed to obtain the envelope spectrum; finally, the entropy spectrum is measured by the envelope spectrum.

The calculation process of envelope spectrum entropy is as follows:

1). The Hilbert transform $h(t) = H(x(t))$ of the signal $x(t)$ is defined as:

$$h(t) = \frac{1}{\pi}\int_{-\infty}^{\infty}\frac{x(\tau)}{t-\tau}d\tau \tag{15}$$

$x(t)$ and $h(t)$ can form a new complex signal:

$$z(t) = x(t) + jh(t) \tag{16}$$

The envelope signal is defined as:

$$E(t) = |z(t)| = \sqrt{x^2(t) + h^2(t)} \tag{17}$$

2). Solve the envelope spectrum. Through the envelope demodulation analysis, the envelope signal can be obtained, and then the obtained envelope signal is FFT transformed to obtain the envelope spectrum. The envelope spectrum analysis can effectively extract the fault frequency component in the rolling bearing vibration signal.

3). Calculate the envelope spectral entropy.

$$\left.\begin{aligned} H_e &= -\sum_{i=1}^{N} p_i \cdot \ln p_i \\ p_i &= HX(i) \Big/ \sum_{j=1}^{N} HX(j) \\ \sum_{i=1}^{N} p_i &= 1 \end{aligned}\right\} \tag{18}$$

where P_i represents the proportion of the spectral value of the i-th point of the envelope spectral entropy in the whole spectrum, and $i = 1, 2, \ldots, n$, n is the number of envelope spectral points. $HX(i)$ is the envelope spectrum of the vibration signal $\{x_i\}, i = 1, 2, \cdots, N$, and H_e is the envelope spectrum entropy. The normalized envelope spectral entropy is given by Eq. (13).

Figure 9 shows the change curve of BLS and MI with the increase of pulse number of periodic impulse signal. It can be seen that as the number of pulses increases, the value of BLS is reduced and has a good ability to characterize the periodicity of the signal; The variation of MI with the increase of the number of pulses is small, indicating that the sensitivity of BLS to the number of pulses is better than MI, so BLS is used as an index to describe the number of signal pulses. Figure 10 shows the variation of MI and BLS as the noise intensity increases. It can be seen from the Figure that the MI change rate is larger than BLS as the noise intensity changes. Therefore, MI is selected as the index for evaluating the noise intensity. In order to effectively evaluate the signal periodicity and noise intensity at the same time, this paper constructs a new index MBLS to evaluate the signal.

Figure 11 is a graph showing the variation of MBLS with the number of pulses. It can be seen that the amplitude of MBLS is decreasing as the number of pulses increases. Figure 12 shows the variation of MBLS with increasing noise

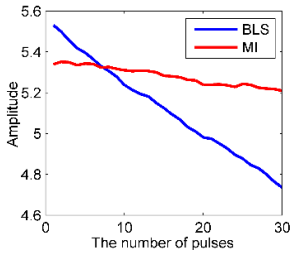

FIGURE 9. Variation curves of BLS and MI with the increase of pulse number.

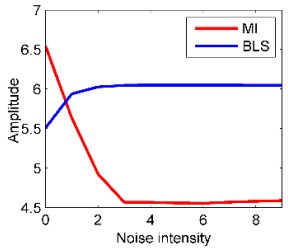

FIGURE 10. Variation curve of BLS and MI when noise intensity increases.

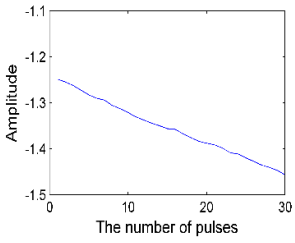

FIGURE 11. Effect of pulse number change on MBLS changes.

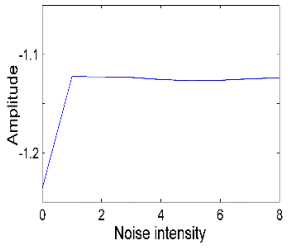

FIGURE 12. Effect of noise intensity change on MBLS.

intensity. It can be seen that as the noise increases, its amplitude first increases and then stabilizes. It can be seen from the Figure that MBLS has a good ability to characterize the number of pulses and the change of noise intensity. Therefore, this paper evaluates the advantages and disadvantages of MSGloG filter parameters by using MBLS as the evaluation index.

B. CHAOTIC GREY WOLF OPTIMIZATION (CGWO)

GWO is a new intelligent algorithm proposed by Seyedali Mirjalili in 2014. This algorithm simulates the characteristics and hierarchy of wolves in the hunting process. By constantly searching and updating the location of prey, eventually, find the prey and initiate a siege on the prey [30]. In the optimization of the combination problem, the performance of the grey wolf algorithm is better than the existing common particle swarm algorithm, gravity search algorithm, differential evolution and other methods. However, the grey Wolf algorithm also has defects. In the process of continuous iteration, the problem of local optimal solution often occurs due to insufficient population diversity. Therefore, the original grey wolf algorithm is improved by introducing a chaotic mapping theory.

In the grey wolf algorithm, the wolves are classified into α wolves, β wolves, δ wolves and remaining wolves ω according to the level, and the position of the prey corresponds to the global optimal solution. α wolf is the head wolf, responsible for leading and managing the entire wolf group and maintaining wolf group discipline, making decisions about whether to prey during the hunting process and controlling the hunting process and working hours. The β wolf is a candidate for the head wolf, and the feedBack information of other wolves is transmitted to the wolf. The δ wolf is responsible for ruling the ω wolves and protecting the safety and integrity of the wolves. The individual ω wolf is responsible for receiving the α wolf search for prey commands and searching for prey.

When the wolves search for the prey, the ω wolf is responsible for searching and feeding back information to the β wolf. The β wolf gets the information to the α wolf. The α wolf gets the information and orders the wolf to move toward the prey. After moving to the ω wolf position, judge whether the prey is found. If it is not found, repeat the steps after the ω wolf performs the prey search until the prey is found. In the hunting process, the distances of α wolf, β wolf, and δ wolf from ω wolf are $D\alpha$, $D\beta$, and $D\delta$. The distance can be calculated by Eq. (19), and the prey position can be calculated by Eq. (20).

$$\begin{aligned} D_\alpha &= |C_1 \cdot X_\alpha - X| \\ D_\beta &= \left|C_2 \cdot X_\beta - X\right| \\ D_\delta &= |C_3 \cdot X_\delta - X| \\ X_1 &= X_\alpha - A_1 \cdot D_\alpha \\ X_2 &= X_\beta - A_2 \cdot D_\beta \\ X_3 &= X_\delta - A_3 \cdot D_\delta \end{aligned} \tag{19, 20}$$

among them:

$$A = 2ar_1 - a \tag{21}$$

$$C = 2r_2 \tag{22}$$

The update location is:

$$X(l+1) = (X_1 + X_2 + X_3)/3 \tag{23}$$

C_1, $C2$ and $C3$ are all calculated by Eq. (22) and are constant variables. The purpose is to set the degree of difficulty of α wolf, β wolf and δ wolf in hunting prey respectively. X is the location of ω wolf; X_1, X_2, X_3 are the location of α wolf, β wolf and δ wolf; A_1, A_2, A_3 are calculated by Eq. (21) and are constant variables; a is the convergence factor, which decreases linearly from 2 to 0 in the iteration process; r_1 and r_2 are random variables of [0, 1], so that grey wolf can search for prey in any direction; $X(l+1)$ is the predicted location for the next generation of prey.

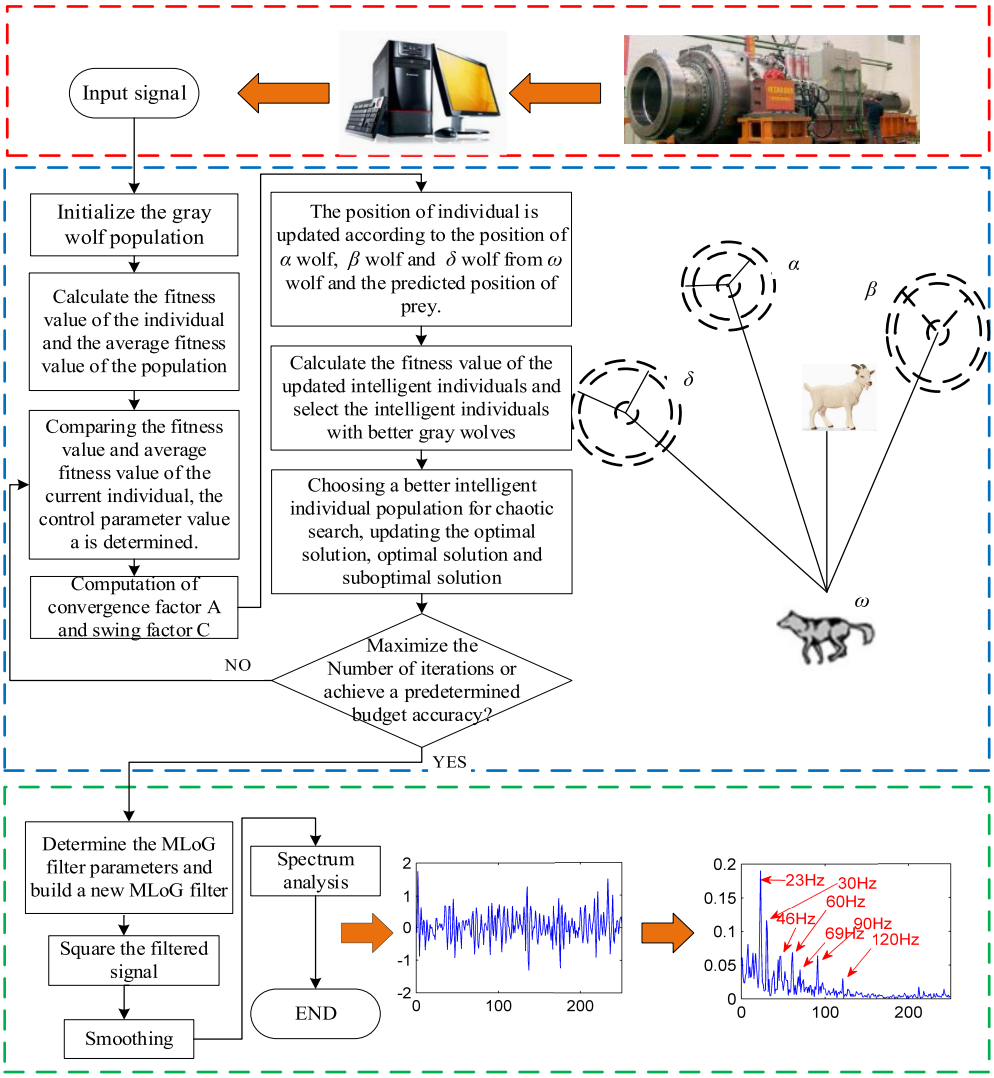

FIGURE 13. Fault diagnosis flow chart of the new MLoG filter.

By adjusting the values of A and C, wolves can reach any position in their area. After each iteration, the location of the next prey is updated. As the convergence factor decreases, the location of the grey wolf approximates the range of prey activity. Through continuous updating and searching, the prey is finally finding the prey and get the global optimal solution. When the GWO algorithm initializes the population, the diversity of the population has a great influence on the iterative optimization of the subsequent generations. Improvement of initialization of grey wolf population using chaotic sequence Logistic map, enriches the diversity of the grey wolf population and speeds up the optimization speed of the grey wolf algorithm. Chaotic maps have a positive impact on the convergence speed of the GWO algorithm because these maps cause chaos in the feasible domain of independent variables. Chaotic can be predicted only in a very short initial time, but is random in a long time. The logistic model expression is:

$$x_n = (m_n - l_n)y_n + l_n \tag{24}$$

where l_n and m_n are the minimum and maximum values of the independent variable x_n;

y_n is a chaotic variable. The initial population after chaos is more uniform than the initial population distribution without chaos, which increases the diversity of the population. In the process of algorithm optimization, the evenly distributed population is easier to find the optimal solution in the global search.

C. PROCESS OF THE PROPOSED METHOD

In this paper, a new fault diagnosis method is proposed. The flowchart of the proposed fault diagnosis method is shown in Figure 13. The marginal envelope spectral entropy index is used as the objective function of the MSGloG method. The method has parameter adaptability. The parameters are optimized by CGWO algorithm. The specific steps are as follows:

(1). Enter the collected mechanical vibration signal. Select the range of MSGloG parameters to be optimized, and

initialize the CGWO parameters, including the maximum number of iterations L and the grey wolf population size N.

(2). Using MSGloG to filter the acquired vibration signal and calculate its fitness. Save the minimum fitness of each iteration of MSGloG.

(3). Determine whether the termination condition is reached. If it is reached, end the iteration. Otherwise, continue the iteration.

(4). Get and record the optimal parameters and minimum fitness.

(5). The original signal is smoothed by the MSGloG method with optimized parameters.

(6). The faulty feature extraction of the processed signal is further performed by the envelope spectrum

IV. SIMULATION VERIFICATION

Due to the harsh working environment, failures of bearing components in wind turbine gearboxes often occur. The fault occurs in the form of periodic shock pulses during signal acquisition. In order to verify the effectiveness and superiority of the proposed method in composite fault detection, a simulation model with two shock signals is constructed. The construction of specific signals is shown in Eq. (25).

$$\begin{aligned} x_1(t) &= A_{m1} \times \exp(-\frac{g}{T_{m1}}) \sin(2\pi f_a t) \\ x_2(t) &= A_{m2} \times \exp(-\frac{g}{T_{m2}}) \sin(2\pi f_a t) \\ x_3(t) &= x_1(t) + x_2(t) + noise \end{aligned} \tag{25}$$

Among them, $x(t)$ is a periodic impact signal. A_{m1} and A_{m2} represent the amplitude of the pulse, g is the damping coefficient, T_{m1} and T_{m2} are the periods of the impact, and f_a is the natural frequency of the axis. The parameter is set to: $g = 0.1, T_{m1} = 1/14, T_{m2} = 1/100, f_a = 260Hz$.

Figure14 is a simulation model diagram, Figure 14(a) is the impact signal $x_1(t)$, Figure 14(b) is the impact signal $x_2(t)$, and Figure 14(c) the waveform diagram of the impact signal contaminated by noise.

In this paper, the chaotic grey wolf algorithm is used to search the marginal envelope spectrum entropy minimum to determine the scale parameter and the sample length of the

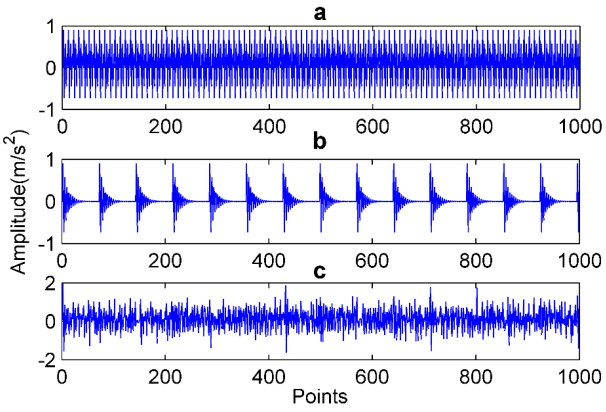

FIGURE 14. Simulation signal time-domain diagram.

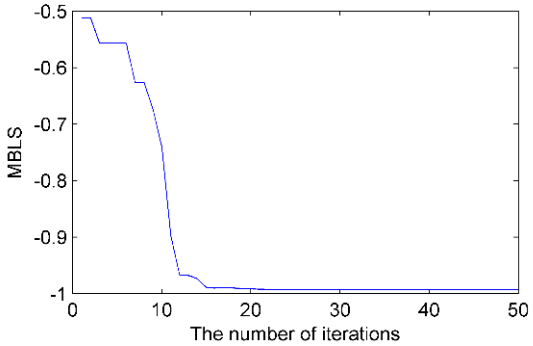

FIGURE 15. Iterative diagram of the chaotic grey wolf algorithm.

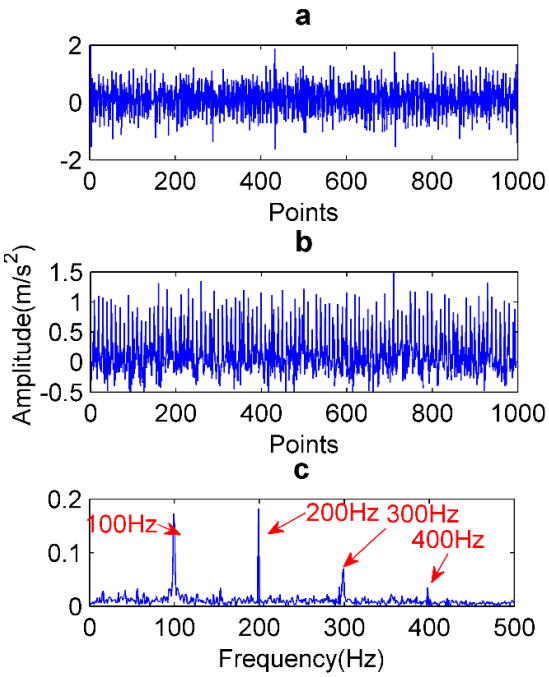

FIGURE 16. Time-domain and frequency-domain diagrams of MED complex signal extraction.

sliding window. The iteration number of the algorithm is 50, and the population is 30. The iterative result of the chaotic grey wolf algorithm is shown in Figure 15. It can be seen from the iteration diagram that the marginal envelope entropy chaotic grey Wolf algorithm proposed in this paper has good convergence. Finally, the scale parameter $\sigma = 0.8$ and the filtering order $k = 3$ are determined by using the method proposed in this paper.

In this paper, the same composite fault simulation model is constructed and the commonly used deconvolution algorithm MED, MOMEDA and autoregressive filtering method (AR) are compared with the proposed method. Figure 16 (a), Figure 17 (a), Figure 18 (a), Figure 19 (a) and Figure 20 (a) are all time-domain waveforms of the original signal. Figure16 shows the extraction result of MED on the simulation model. According to [31], the filter length of MED is L=15. Figure16(b) is the filtering result of MED on the simulation model after optimizing the filter length.

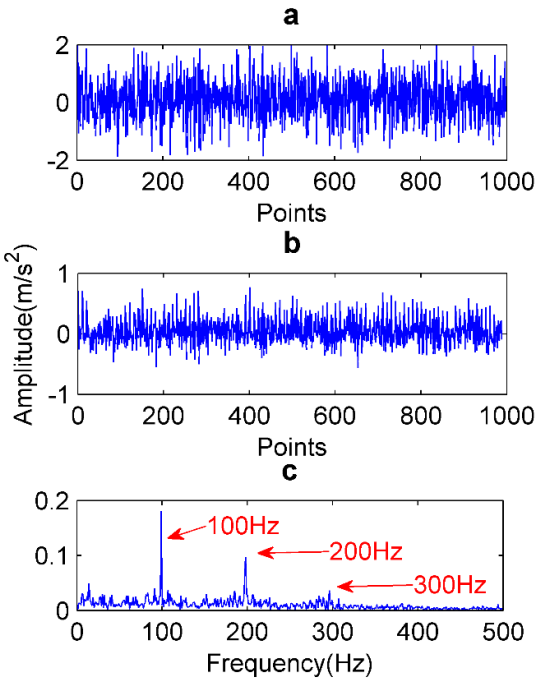

FIGURE 17. Time-domain and frequency-domain diagrams of MOMEDA complex signal extraction.

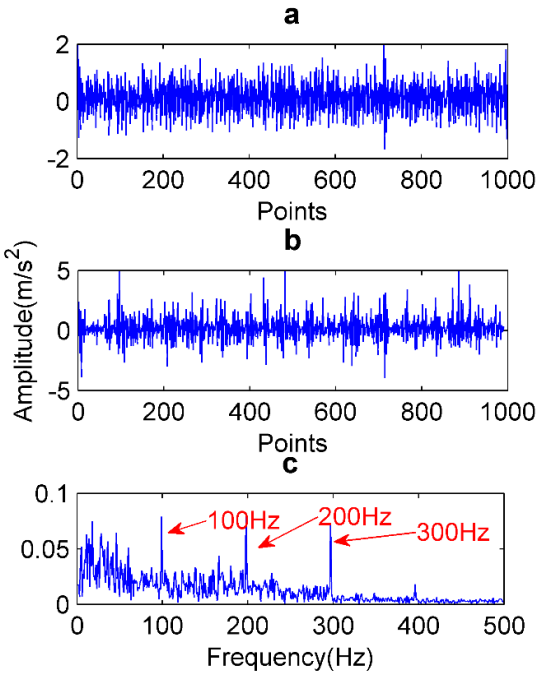

FIGURE 18. Time-domain and frequency-domain diagrams of AR complex signal extraction.

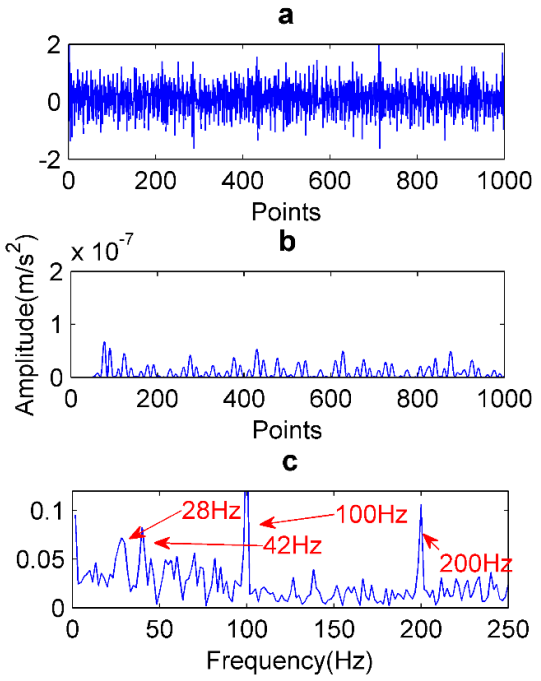

FIGURE 19. Time-domain and frequency-domain diagrams of MIoG complex signal extraction.

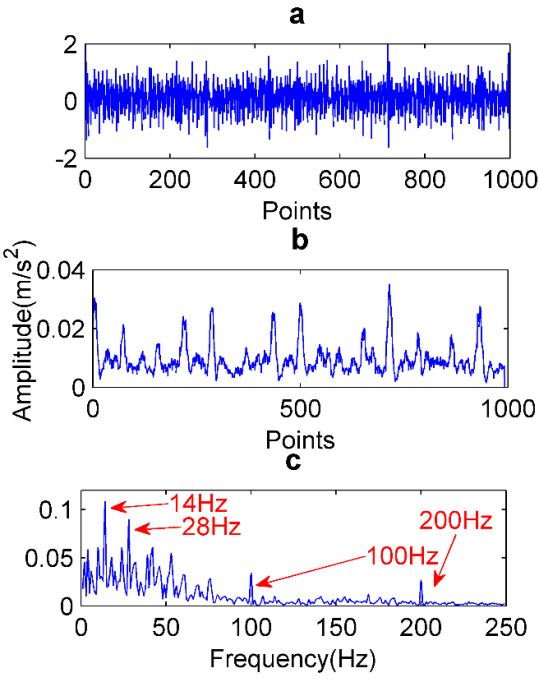

FIGURE 20. Time-domain and frequency-domain diagrams of MSGIoG complex signal extraction.

Figure16(c) is the frequency domain result of the envelope spectrum extraction of MED filtering results. It can be seen from the Figure that the MED has a good extraction ability for the high-frequency signal in the composite signal, but the extraction effect on the low-frequency signal is not good. Figure17 is a diagram showing the extraction results of the simulated signal by MOMEDA. According to [19], the filter length is selected as L=50. Figure17(b) is the filtering result of the composite fault simulation model by the MOMEDA method; Figure17(c) is an envelope spectrum analysis waveform for filtering the time domain results of the MOMEDA filter. It can be seen from the Figure that MOMEDA has limitations on the diagnostic analysis results of the composite signals. It can effectively identify the fault frequency of 100Hz, but does not extract the fault frequency Figure18

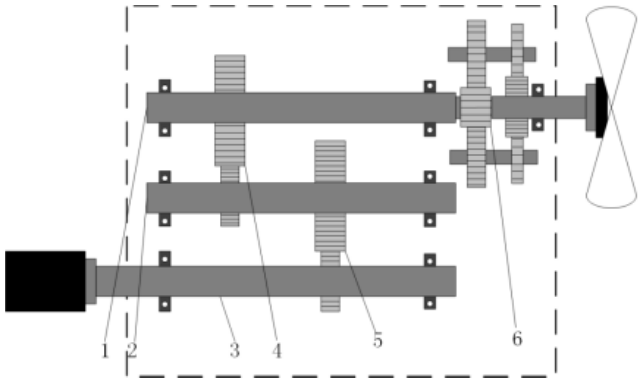

1- Intermediate shaft ; 2- Low speed shaft ; 3- High speed shaft ; 4- Medium speed gear ; 5- High speed gear ; 6- Planetary gear

FIGURE 21. Wind power gearbox test bench.

a. Wind power gearbox bearing inner ring peeling off

b. Wind turbine gearbox bearing rolling element pitting

FIGURE 22. Wind turbine gearbox bearing inner ring and rolling element fault diagram.

of 14Hz. is an extracted waveform diagram of the AR simulation model, Figure18(b) is a waveform diagram after AR filtering; Figure 18(c) is an envelope spectrum analysis waveform of the composite signal after AR filtering. It can effectively extract the fault frequency of 100Hz, but it has some limitations in the identification of low-frequency faults. Figure19 is a waveform diagram of the simulation model of the composite fault in the original MloG method. Figure19(b) shows the waveform diagram of the original composite signal processed by MloG smoothing and Figure19(c) is a waveform diagram of frequency domain analysis of the MloG filtered signal. The frequency domain analysis of the waveform shows that the two and three times of 14Hz are extracted, but the pulse information of 14Hz cannot be obviously observed.The fault characteristic information of 100Hz is extracted effectively. Figure 20 is a waveform diagram of the composite fault diagnosis of the simulated signal by the method MSGloG proposed in this paper, Figure 20(b) shows the time domain waveform after smoothing filtering. Figure 20(c) is a frequency spectrum of the signal processed by the MSGloG method, in which both fault frequencies are effectively extracted, and the extracted fault feature frequency is more significant. The proposed method of MSGloG is better than the commonly used fault extraction deconvolution method MED, MOMEDA, MloG and autoregressive filtering method AR in the extraction of multi-fault simulation models.

V. EXPERIMENTAL VERIFICATION

In order to verify the feasibility of the proposed method in engineering application, the proposed method is applied to the composite fault diagnosis of wind turbine gearbox. In Figure 21, the structure of a wind turbine gearbox test bench is shown. The main components of the test bench include motors, wind turbines, acceleration sensors, data acquisition analyzers, gearboxes, etc. At the same time, the output shaft has a frequency of 30.24 Hz, the intermediate shaft has a frequency of 8.19 Hz, the low- speed axis has a frequency of 1.8 Hz, and the data sampling frequency is 5000 Hz. The frequency of failures can be obtained by calculation. The specific failure information is listed in Table 1. Figure 22 shows the failure diagram of the wind turbine gearbox bearing and rolling elements. The fault type of gearbox in this experiment is a composite fault. Figure 22 (a) is the bearing inner ring peeling failure, Figure 22 (b) is the pitting failure of the bearing rolling element.

Figure 23 is a waveform diagram of the collected measured fault signal and an envelope spectrum waveform of the signal. It can be seen from the figure that the double frequency, triple frequency and quadruple frequency of the inner ring fault frequency are effectively extracted, but the fault characteristic information of the rolling element is not extracted effectively. Therefore, it is particularly important to enhance the fault characteristics of the signal.

TABLE 1. Fault frequency.

Intermediate shaft speed *n*	Intermediate shaft frequency shift	Inner ring failure frequency	Rolling element failure frequency
491.4rpm	8.19Hz	84.3Hz	27.3Hz

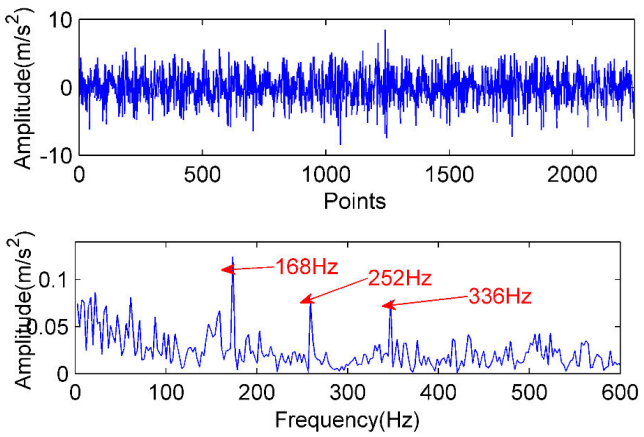

FIGURE 23. Vibration signal diagram of wind power gearbox measured.

Figure 24 is the result of fault information extraction in the experimental signal by MOMEDA algorithm. Figure 24(a) is the collected original signal. Figure 24(b) shows the fault information obtained by the deconvolution of the original signal by the MOMEDA algorithm. In the Figure, it can be seen that the impact information is highlighted; Figure 24(c) is the frequency domain diagram of the envelope spectrum extraction of the experimental signal processed by MOMEDA, which can be visually seen from the Figure, the fault information of the inner ring of the bearing is effectively extracted, but the fault information of the rolling element is still submerged by the noise and is not effectively extracted.

Figure 25 is the result of fault information extraction in the experimental signal by AR algorithm. Figure 25(a) is a waveform diagram of the original vibration signal of the collected wind power gearbox; Figure 25(b) is a time-domain waveform diagram obtained by performing AR filtering on the collected vibration signal; Figure 25(c) is the envelope signal diagram of the vibration signal of the wind power gearbox after filtering by the AR algorithm. In the Figure, the fault information of the inner ring of the bearing is still effectively extracted, and the effect of extracting the fault information of the rolling element is not obvious.

Figure 26 is the result of fault information extraction in the experimental signal by MED algorithm. The MED algorithm can enhance the amplitude of the shock information while filtering the vibration signal. Figure 26(a) is the vibration signal of the collected wind turbine gearbox; Figure 26(b) is the time-domain diagram of the fault information after filtering the acquired signal by MED algorithm; Figure 26(c) is the envelope spectrum analysis of the vibration signal after MED

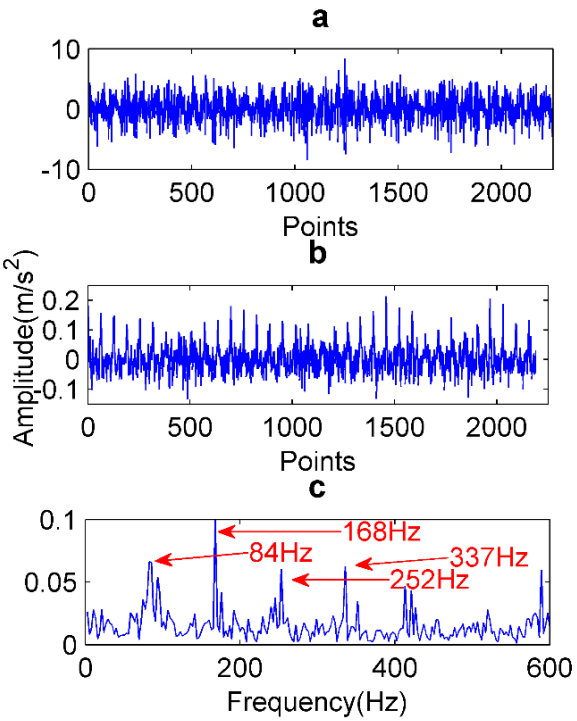

FIGURE 24. MOMEDA processing results of measured signals.

processing. It can be seen intuitively from the Figure that the extraction effect of the bearing inner ring fault is obvious and the rolling element fault feature information is not effectively extracted.

Figure 27 is the result of fault information extraction in the experimental signal by MloG algorithm. Using the method proposed in this paper, the scale parameter of the experimental signal is determined to be $\sigma = 1.2$. Figure 27(a) is the vibration information of the wind turbine gearbox collected in the experiment; Figure 27(b) is a waveform diagram of the smoothed filtering of the acquired vibration signal waveform by the MloG algorithm. It is clear that the noise information contained in the vibration signal is attenuated; Figure 27(c) is a waveform diagram of the envelope spectrum processing of the vibration information after smooth filtering by MloG. It can be seen that there are two frequencies related to the failure of the rolling element, while there is only one frequency related to the failure of the bearing inner ring. Such a fault extraction result is not very satisfactory.

Figure 28 is the result of fault information extraction in the experimental signal by MSGlog algorithm. Using the method proposed in this paper, the scale parameter of the experimental signal is determined to be $\sigma = 1.2$ and the filter order

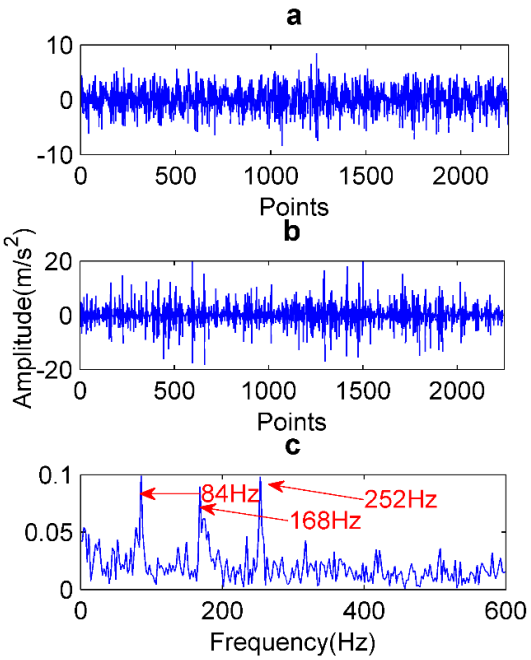

FIGURE 25. AR processing results of measured signals.

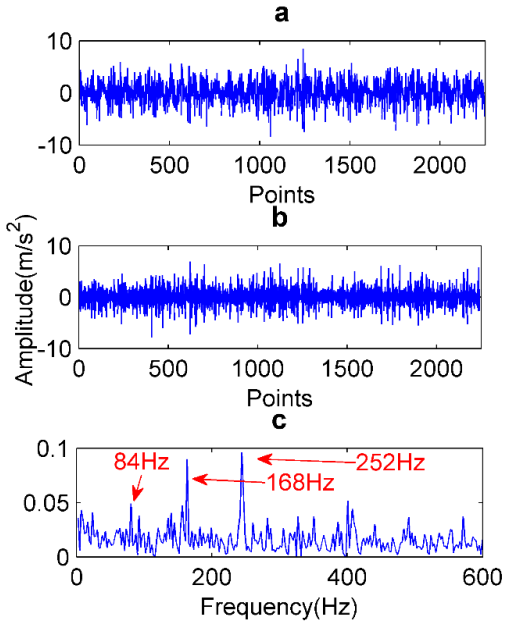

FIGURE 26. MED processing results of measured signals.

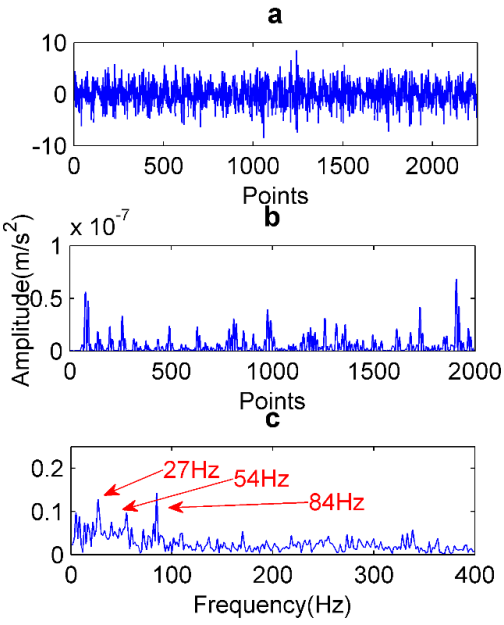

FIGURE 27. MloG processing results of measured signals.

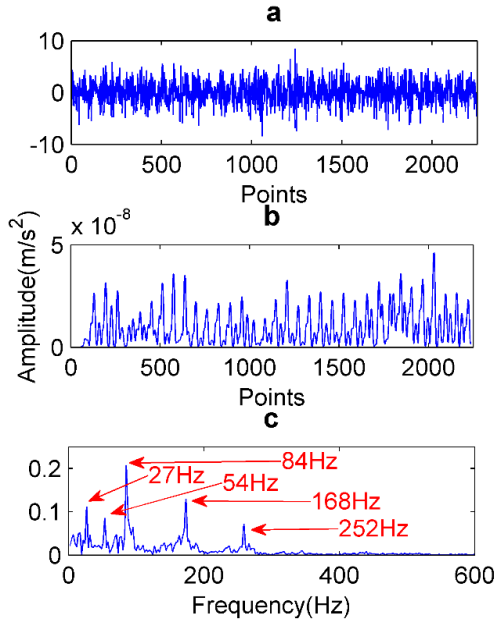

FIGURE 28. MSGloG processing results of measured signals.

$k = 3$. Figure 28(a) is the vibration information of the wind turbine gearbox collected in the experiment; Figure 28(b) is a waveform diagram of the smoothed filtering of the acquired vibration signal waveform by the MSGloG algorithm. Figure 28(c) is a waveform diagram of the envelope spectrum processing of the vibration information after smooth filtering by MSGloG. It can be seen that the fault frequency of the rolling element is effectively extracted, the frequency multiplication of the fault is clearly displayed, and the fault characteristic information of the inner ring fault of the bearing is effectively extracted, the purpose of extracting multiple fault features of wind power gearbox is achieved.

VI. CONCLUSION

The improved Gaussian filtering method has certain advantages compared with the existing deconvolution method and the autoregressive filtering algorithm, but the filter order and scale parameters have a great influence on the effect of the method. This paper proposes a new indicator for evaluating the MSGloG effect, the marginal envelope spectral entropy, this index can simultaneously evaluate the periodicity of the signal and the noise reduction performance of the Gaussian

filtering method. By discriminating the index, the two parameters that affect the filtering effect can be reasonable. Through simulation verification, the proposed marginal envelope spectral entropy index can well evaluate the effect of MSGloG.

This paper proposes an adaptive MSGloG fault diagnosis method based on marginal envelope spectral entropy, which is successfully applied to the composite fault diagnosis of wind turbine gearbox. Through simulation and experimental analysis, the proposed method is superior to the current common methods in the extraction of composite faults for wind turbine gearboxes.

REFERENCES

[1] Z. Qiao, Y. Lei, and N. Li, "Applications of stochastic resonance to machinery fault detection: A review and tutorial," *Mech. Syst. Signal Process.*, vol. 122, pp. 502–536, May 2019, doi: 10.1016/j.ymssp.2018.12.032.

[2] B. Cai, X. Shao, Y. Liu, X. Kong, H. Wang, H. Xu, and W. Ge, "Remaining useful life estimation of structure systems under the influence of multiple causes: Subsea pipelines as a case study," *IEEE Trans. Ind. Electron.*, vol. 67, no. 7, pp. 5737–5747, Jul. 2020, doi: 10.1109/TIE.2019.2931491.

[3] H. Wang, B. Ren, L. Song, and L. Cui, "A novel weighted sparse representation classification strategy based on dictionary learning for rotating machinery," *IEEE Trans. Instrum. Meas.*, vol. 69, no. 3, pp. 712–720, Mar. 2020, doi: 10.1109/TIM.2019.2906334.

[4] B. Cai, H. Liu, and M. Xie, "A real-time fault diagnosis methodology of complex systems using object-oriented Bayesian networks," *Mech. Syst. Signal Process.*, vol. 80, pp. 31–44, Dec. 2016, doi: 10.1016/j.ymssp.2016.04.019.

[5] Y. Lei, Z. Qiao, X. Xu, J. Lin, and S. Niu, "An underdamped stochastic resonance method with stable-state matching for incipient fault diagnosis of rolling element bearings," *Mech. Syst. Signal Process.*, vol. 94, pp. 148–164, Sep. 2017, doi: 10.1016/j.ymssp.2017.02.041.

[6] Z. Wang, Z. Han, F. Gu, J. X. Gu, and S. Ning, "A novel procedure for diagnosing multiple faults in rotating machinery," *ISA Trans.*, vol. 55, pp. 208–218, Mar. 2015, doi: 10.1016/j.isatra.2014.09.006.

[7] Y. Wang, G. Xu, L. Liang, and K. Jiang, "Detection of weak transient signals based on wavelet packet transform and manifold learning for rolling element bearing fault diagnosis," *Mech. Syst. Signal Process.*, vols. 54–55, pp. 259–276, Mar. 2015, doi: 10.1016/j.ymssp.2014.09.002.

[8] B. P. Cai, Y. Liu, and M. Xie, "A dynamic-Bayesian-network-based fault diagnosis methodology considering transient and intermittent faults," *IEEE Trans. Automat. Sci. Eng.*, vol. 14, no. 1, pp. 276–285, Jan. 2017, doi: 10.1109/TASE.2016.2574875.

[9] J. Zheng, H. Pan, S. Yang, and J. Cheng, "Generalized composite multiscale permutation entropy and Laplacian score based rolling bearing fault diagnosis," *Mech. Syst. Signal Process.*, vol. 99, pp. 229–243, Jan. 2018, doi: 10.1016/j.ymssp.2017.06.011.

[10] L. Song, H. Wang, and P. Chen, "Step-by-step fuzzy diagnosis method for equipment based on symptom extraction and trivalent logic fuzzy diagnosis theory," *IEEE Trans. Fuzzy Syst.*, vol. 26, no. 6, pp. 3467–3478, Dec. 2018, doi: 10.1109/TFUZZ.2018.2833820.

[11] H. Liu, W. Huang, S. Wang, and Z. Zhu, "Adaptive spectral kurtosis filtering based on Morlet wavelet and its application for signal transients detection," *Signal Process.*, vol. 96, pp. 118–124, Mar. 2014, doi: 10.1016/j.sigpro.2013.05.013.

[12] Y. Li, G. Li, Y. Yang, X. Liang, and M. Xu, "A fault diagnosis scheme for planetary gearboxes using adaptive multi-scale morphology filter and modified hierarchical permutation entropy," *Mech. Syst. Signal Process.*, vol. 105, pp. 319–337, May 2018, doi: 10.1016/j.ymssp.2017.12.008.

[13] Z. Wang, J. Zhou, J. Wang, W. Du, J. Wang, X. Han, and G. He, "A novel fault diagnosis method of gearbox based on maximum kurtosis spectral entropy deconvolution," *IEEE Access*, vol. 7, pp. 29520–29532, 2019, doi: 10.1109/ACCESS.2019.2900503.

[14] Y. Lei, J. Lin, Z. He, and M. J. Zuo, "A review on empirical mode decomposition in fault diagnosis of rotating machinery," *Mech. Syst. Signal Process.*, vol. 35, nos. 1–2, pp. 108–126, Feb. 2013, doi: 10.1016/j.ymssp.2012.09.015.

[15] Z. Wang, J. Wang, W. Cai, J. Zhou, W. Du, J. Wang, G. He, and H. He, "Application of an improved ensemble local mean decomposition method for gearbox composite fault diagnosis," *Complexity*, vol. 2019, pp. 1–17, May 2019, doi: 10.1155/2019/1564243.

[16] C. Shen, J. Yang, J. Tang, J. Liu, and H. Cao, "Note: Parallel processing algorithm of temperature and noise error for micro-electro-mechanical system gyroscope based on variational mode decomposition and augmented nonlinear differentiator," *Rev. Scientific Instrum.*, vol. 89, no. 7, Jul. 2018, Art. no. 076107, doi: 10.1063/1.5037052.

[17] X. Jiang, J. Wang, J. Shi, C. Shen, W. Huang, and Z. Zhu, "A coarse-to-fine decomposing strategy of VMD for extraction of weak repetitive transients in fault diagnosis of rotating machines," *Mech. Syst. Signal Process.*, vol. 116, pp. 668–692, Feb. 2019, doi: 10.1016/j.ymssp.2018.07.014.

[18] R. A. Wiggins, "Minimum entropy deconvolution," *Geoexploration*, vol. 16, pp. 21–35, Apr. 1980, doi: 10.1016/0016-7142(78)90005-4.

[19] Y. Cheng, Z. Wang, W. Zhang, and G. Huang, "Particle swarm optimization algorithm to solve the deconvolution problem for rolling element bearing fault diagnosis," *ISA Trans.*, vol. 90, pp. 244–267, Jul. 2019, doi: 10.1016/j.isatra.2019.01.012.

[20] Y. Cheng, Z. Wang, B. Chen, W. Zhang, and G. Huang, "An improved complementary ensemble empirical mode decomposition with adaptive noise and its application to rolling element bearing fault diagnosis," *ISA Trans.*, vol. 91, pp. 218–234, Aug. 2019, doi: 10.1016/j.isatra.2019.01.038.

[21] G. L. McDonald and Q. Zhao, "Multipoint optimal minimum entropy deconvolution and convolution fix: Application to vibration fault detection," *Mech. Syst. Signal Process.*, vol. 82, pp. 461–477, Jan. 2017, doi: 10.1016/j.ymssp.2016.05.036.

[22] Z. Wang, W. Du, J. Wang, J. Zhou, X. Han, Z. Zhang, and L. Huang, "Research and application of improved adaptive MOMEDA fault diagnosis method," *Measurement*, vol. 140, pp. 63–75, Jul. 2019, doi: 10.1016/j.measurement.2019.03.033.

[23] X. Yan and M. Jia, "Application of CSA-VMD and optimal scale morphological slice bispectrum in enhancing outer race fault detection of rolling element bearings," *Mech. Syst. Signal Process.*, vol. 122, pp. 56–86, May 2019, doi: 10.1016/j.ymssp.2018.12.022.

[24] N. Sawalhi, W. Wang, and A. Becker, "Vibration signal processing for spall size estimation in rolling element bearings using autoregressive inverse filtration combined with bearing signal synchronous averaging," *Adv. Mech. Eng.*, vol. 9, no. 5, May 2017, Art. no. 168781401770300, doi: 10.1177/1687814017703007.

[25] J.-L. Liu and D.-Z. Feng, "Two-dimensional multi-pixel anisotropic Gaussian filter for edge-line segment (ELS) detection," *Image Vis. Comput.*, vol. 32, no. 1, pp. 37–53, Jan. 2014, doi: 10.1016/j.imavis.2013.12.001.

[26] X. Zhang, Q. Miao, Z. Liu, and Z. He, "An adaptive stochastic resonance method based on grey wolf optimizer algorithm and its application to machinery fault diagnosis," *ISA Trans.*, vol. 71, pp. 206–214, Nov. 2017, doi: 10.1016/j.isatra.2017.08.009.

[27] Z. J. Teng, J. L. Lv, and L. W. Guo, "An improved hybrid grey wolf optimization algorithm," *Soft Comput.*, vol. 23, pp. 6617–6631, Aug. 2019, doi: 10.1007/s00500-018-3310-y.

[28] D. Marr and E. Hildreth, "Theory of edge detection," *Proc. Roy. Soc. London. B. Biol. Sci.*, vol. 207, pp. 187–217, Feb. 1980, doi: 10.1098/rspb.1980.0020.

[29] M. Basu, "Gaussian-based edge-detection methods–A survey," *IEEE Trans. Syst., Man Cybern., C (Appl. Rev.)*, vol. 32, no. 3, pp. 252–260, Aug. 2002, doi: 10.1109/TSMCC.2002.804448.

[30] S. Mirjalili, S. M. Mirjalili, and A. Lewis, "Grey wolf optimizer," *Adv. Eng. Softw.*, vol. 69, pp. 46–61, Mar. 2014, doi: 10.1016/j.advengsoft.2013.12.007.

[31] Y. Cheng, N. Zhou, W. H. Zhang, and Z. W. Wang, "Application of an improved minimum entropy deconvolution method for railway rolling element bearing fault diagnosis," *J. Sound Vib.*, vol. 425, pp. 53–69, Jul. 2018, doi: 10.1016/j.jsv.2018.01.023.

NENGQUAN DUAN received the M.S. degree from the North University of China, in 2009. He is currently a Lecturer with the North University of China. His research interests include machine vision and algorithm design.

JINGTAI WANG received the master's degree in mechanical engineering from the North University of China, in 2020. His research interests include mechanical fault diagnosis and signal processing.

TIANSHENG ZHAO graduated in industrial automation from East China Jiaotong University, in 2001. He received the bachelor's degree. He is currently a Senior Engineer with the Zhengzhou Mechanical and Electrical Engineering Research Institute. His research interests include electromechanical control and fault diagnosis techniques.

WENHUA DU received the Ph.D. degree from Tianjin University, Tianjin, China. She was a Visiting Scholar with Warwick University, from 2016 to 2017. She is currently a Professor with the North University of China. Her research interests include mechanical dynamics and machine vision.

XIAOMING GUO received the bachelor's degree in mechanical design and manufacturing and automation from the North University of China, in 2014. He is currently a Graduate Student with the School of Mechanical Engineering, North University of China. His current research field includes composite fault diagnosis of gearboxes.

JUNYUAN WANG received the Ph.D. degree from the Taiyuan University of Technology. He is currently a Professor with the North University of China, the Vice Chairman of the Shanxi Province Society of Vibration Engineering, the Executive Director and Deputy Secretary-General of the Shanxi Province Mechanical Engineering Society, and the Vice Chairman of the Mechanical Transmission Branch of the Shanxi Province Mechanical Engineering Society. His research interest includes intelligent manufacturing technology and systems.